

Serotonergic Modulation of Intrinsic Functional Connectivity

Alexander Schaefer,^{1,2} Inga Burmann,¹ Ralf Regenthal,³ Katrin Arélin,^{1,4,5} Claudia Barth,¹ André Pampel,⁶ Arno Villringer,^{1,4,5,7,8} Daniel S. Margulies,^{8,9} and Julia Sacher^{1,4,8,*}

¹Department of Neurology, Max Planck Institute for Human Cognitive and Brain Sciences, 04103 Leipzig, Germany

²Department of Electrical and Computer Engineering, Clinical Imaging Research Centre & Singapore Institute for Neurotechnology, National University of Singapore, 117583 Singapore, Singapore

³Division of Clinical Pharmacology, Rudolf-Boehm-Institute of Pharmacology and Toxicology, University of Leipzig, 04107 Leipzig, Germany

⁴Clinic of Cognitive Neurology, University Hospital Leipzig, 04103 Leipzig, Germany

⁵Leipzig Research Center for Civilization Diseases, University of Leipzig, 04103 Leipzig, Germany

⁶Nuclear Magnetic Resonance Unit, Max Planck Institute for Human Cognitive and Brain Sciences, 04103 Leipzig, Germany

⁷Integrated Research and Treatment Center Adiposity Diseases, University of Leipzig, 04103 Leipzig, Germany

⁸Berlin School of Mind and Brain, Mind and Brain Institute, Charité and Humboldt University, 10099 Berlin, Germany

⁹Max Planck Research Group for Neuroanatomy & Connectivity, Max Planck Institute for Human Cognitive and Brain Sciences, 04103 Leipzig, Germany

Summary

Serotonin functions as an essential neuromodulator that serves a multitude of roles, most prominently balancing mood [1]. Serotonergic challenge has been observed to reduce intrinsic functional connectivity in brain regions implicated in mood regulation [2–4]. However, the full scope of serotonergic action on functional connectivity in the human brain has not been explored. Here, we show evidence that a single dose of a serotonin reuptake inhibitor dramatically alters functional connectivity throughout the whole brain in healthy subjects ($n = 22$). Our network-centrality analysis reveals a widespread decrease in connectivity in most cortical and subcortical areas. In the cerebellum and thalamus, however, we find localized increases. These rapid and brain-encompassing connectivity changes linked to acute serotonin transporter blockade suggest a key role for the serotonin transporter in the modulation of the functional macroscale connectome.

Results and Discussion

Serotonin is a key neuromodulator and plays an important role in balancing mood, cognitive control, many endocrine and autonomic processes, and sensorimotor output and perception [1]. Serotonergic projections innervate a multitude of cortical and subcortical brain regions [5]. However, the extent to which the brain's intrinsic functional connectivity can be

altered by an acute serotonergic challenge is not known. The serotonin transporter (5-HTT) is essential for maintaining adequate brain serotonin homeostasis, and alteration of its function has been linked to heightened susceptibility for depression and anxiety [6–8]. It is also the main target of action for selective serotonin reuptake inhibitors (SSRIs), the most widely prescribed class of antidepressants worldwide [9]. Administration of an acute dose of an SSRI has been shown to raise serotonin levels in frontal cortex, striatum, hippocampus, and raphe nucleus [10–12]. This effect is regularly used to investigate the consequences of acutely enhanced serotonergic transmission in the human brain in vivo [13–15]. In vivo neurochemical imaging of the human brain on an employable timescale has been a methodological challenge. However, investigating the alterations in global connectivity induced by a pharmacological modulation using noninvasive rs-fMRI offers a window to elucidating the link between neurochemical systems and intrinsic brain organization. Resting-state functional magnetic resonance imaging (rs-fMRI) focuses on the assessment of spontaneous low-frequency fluctuations in the absence of any task [16]. Connectivity measures between these spontaneous fluctuations in brain activity have been observed to reflect communication across large-scale networks in the human brain [17–19]. The capacity of serotonin to impact functional connectivity in specific areas of the human brain has recently been demonstrated [2–4] but the full potential of rs-fMRI to advance our understanding of how serotonin and functional connectivity changes relate has not yet been explored. Previous reports on SSRI-induced functional connectivity changes by rs-fMRI were restricted to single-seed [2, 3] or single-network [4] analysis. Our aims in the current study were to investigate whether the impact of SSRI-induced change in functional connectivity extends to the entire human brain and to explore whether such a whole-brain connectivity change is in fact a consistent decrease as previous research indicates [2–4].

Given the widespread distribution of the serotonergic system, we hypothesized that an acute serotonergic challenge would have a large-scale impact on the intrinsic functional connectivity of most cortical and subcortical areas and should not be limited to specific networks. To this end, we measured changes in connectivity using degree centrality [20] in antidepressant-naïve and medication-free volunteers ($n = 22$; 11 females; age, 25; SD, 2) who engaged in a double-blind, placebo-controlled, two-way cross-over design (for overview, see Figure 1; for details on study design, image processing, and analysis, see Supplemental Experimental Procedures available online) and underwent three resting-state scanning sessions: after a baseline rs-fMRI scan, participants received either a single oral dose of the study drug escitalopram (20 mg) or placebo in a randomized design (separated by a wash-out period of 8 weeks). MRI scanning was scheduled during the maximum concentration of escitalopram in blood, between 3 and 4 hr [21] after drug administration. Plasma levels of escitalopram were 25 ± 13 ; 16–57 (mean \pm SD; range) ng/ml.

We found a single dose of selective serotonin reuptake inhibitor to spark a widespread connectivity decrease throughout the brain (Figure 2): we report a global synchrony

*Correspondence: sacher@cbs.mpg.de

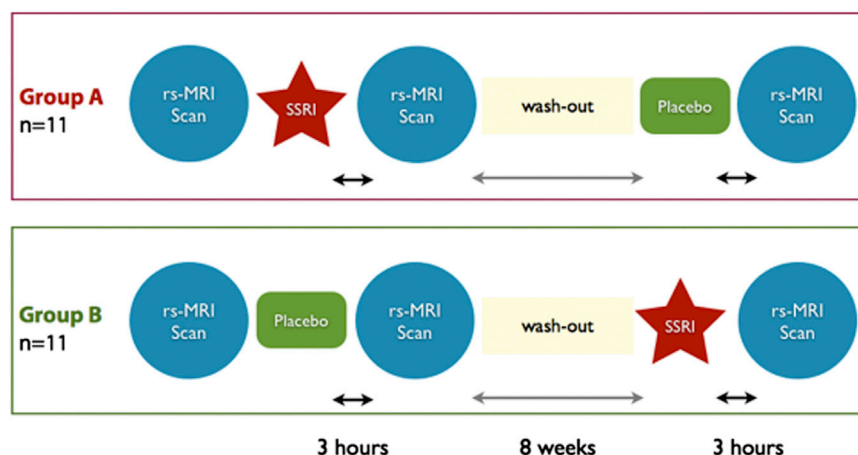


Figure 1. Study Design

Twenty-two subjects underwent three resting-state scanning sessions: after a baseline rs-MRI scan, participants received either a single oral dose of the study drug escitalopram (20 mg) (depicted by a red star) or placebo (depicted by a green rectangle) in a randomized design. Serum levels of escitalopram were determined after 3 hr followed by a second rs-fMRI scan. After a wash-out period of 8 weeks, the protocol was repeated with the alternate study drug (escitalopram or placebo) to adhere to a double-blind intraindividual design. rs-fMRI scans are indicated as blue circles.

change revealing a widespread decrease in connectivity in most cortical and subcortical areas ($p < 0.01$, cluster-corrected) at the peak concentration of a single dose of 20 mg escitalopram (Figure 2). In the placebo condition, we did not find any significant clusters at this threshold. Our analysis also revealed substantial regional differences in connectivity change: we observed localized increases in connectivity from cerebellar and thalamic regions in addition to a connectivity decrease in most cortical and subcortical areas. Figure 3 displays the contrast in degree centrality of escitalopram versus placebo: we report a general decrease in functional connectivity throughout the brain, with the exception of localized increases in cerebellar and thalamic regions ($p < 0.01$, cluster-corrected). Figure S3 depicts the contrast at a range of thresholds ($r > 0.10$, $r > 0.15$, $r > 0.20$). Table S1 provides a comprehensive overview of all significant clusters in the escitalopram versus placebo condition.

To explore a potential influence of escitalopram on signal properties, which could account for the connectivity findings, we computed the power of the resting-state signal [17]. In the analysis of the amplitude of low-frequency fluctuations (ALFF), we did not find any significant changes when contrasting escitalopram to placebo condition. Hence, the signal change depicted in Figure 3 appears to be more specific to the connectivity between regions (for further details on connectivity changes within and between network modules, see Figure S1), providing support for the interpretation of our results as a reflection of an alteration in functional synchronization rather than a loss of power in the resting state signal.

To investigate whether the functional connectivity changes we find reflect short-range or long-range connections, we calculated the distance of each connection. Figure 4 shows that the change in functional connectivity of the majority of connections (reflected in red) occurs within the long-range distance of 6–12 cm. This analysis supports a conceptual framework of serotonergically modulated functional connectivity in long-range circuits. This finding draws further support from electrophysiological data demonstrating serotonin to drive long-range connections from both cerebellar cortex [22] and contralateral cortico-cortical projections [23]. Complimentary analyses of the functional connectivity change mapped on major network modules [24] reveal the change in functional connectivity to span across all major functional networks of the brain (see Figures S1 and S2 and details in Supplemental Data).

We acknowledge that degree centrality is a measure that can be viewed as difficult to relate to function in a specific cognitive domain or a particular aspect of emotional processing. However, there is a consensus among experts [25, 26] that although interpreting intrinsic functional connectivity faces constraints both from static anatomical connectivity and from poorly understood dynamic functional coupling changes [25], this powerful technique provides unique insights into human brain organization. We therefore view our findings as an essential first step for establishing the framework for future behavioral- and task-based studies in clinical populations.

Some of our whole-brain results are consistent with previous seed-based studies indicating functional connectivity decreases following SSRI administration in subcortical and cortical areas [2–4]. However, our findings challenge the view that SSRI-induced changes are limited to decreases in connectivity, as we demonstrate substantial regional differences in connectivity change following escitalopram intake: a series of animal studies find total citalopram concentrations to be twice as high in cortex compared to the citalopram levels in mesencephalon-pons following chronic [27] and single-dose [28] administration. These data are consistent with evidence from human PET studies reporting regional differences in glucose-metabolism changes following acute versus chronic SSRI administration [29], differences in 5-HTT occupancy rates after a single dose of an SSRI [30], as well as differences in acute SSRI effects on endogenous serotonin concentration levels [31] and the regional differences in functional connectivity between cortical and more central brain regions we observe after a single, clinically relevant dose of escitalopram.

In the study by Nord et al. [31], a single dose of escitalopram was found to decrease serotonin in cortical serotonergic projection areas while a trend for an increase in serotonin levels was found in central serotonergic brain regions. This is of particular interest as it had long been hypothesized that extracellular serotonin rises after acute SSRI administration in the entire brain. In light of recent findings supporting a decrease in serotonin levels in cortical projections areas [31], it seems likely that the effect of SSRIs on extracellular serotonin levels differs among brain areas. This observation fits well with our data suggesting that a single dose of escitalopram affects functional connectivity differently in distinct brain areas. Parameters like blood flow, lipophilicity, 5-HTT density, and 5-HTT internalization processes are likely to contribute to those regional differences and we are just beginning to systematically study these regional differences in the context of the time frame of drug administration. A systematic

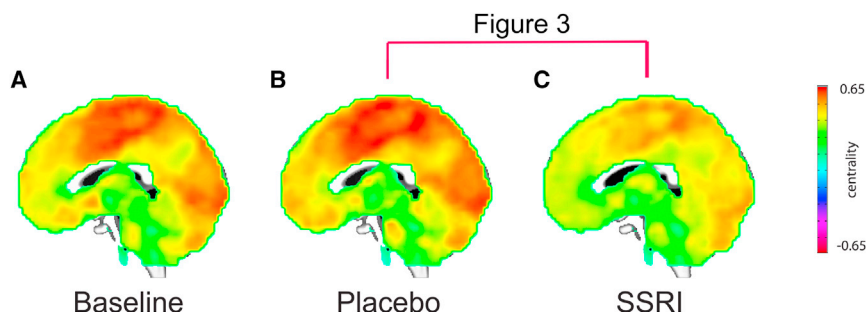


Figure 2. Comparison of Average Degree Centrality Baseline versus Placebo and Escitalopram. Sagittal slices of mean degree centrality of three conditions: (A) baseline, (B) placebo, and (C) escitalopram (20 mg), superimposed on a T1-anatomical standard template. Orange colors indicate higher centrality. Baseline and placebo condition show more similar centrality patterns, whereas degree centrality analysis reveals a global signal change following the administration of the SSRI.

categorization of these regional differences that have been observed for acute, subacute, and chronic effects of SSRI administration on brain metabolism, neurochemistry, and intrinsic connectivity will be needed before the potential of these neural correlates to guide psychopharmacological treatment decisions can be evaluated.

While we observed a widespread decrease in connectivity in most subcortical and cortical areas, localized increases were observed in cerebellar and thalamic regions. The increase in connectivity found in the thalamus and cerebellum may be of particular relevance for the excitability of the many serotonergic projection neurons that terminate in the thalamus [32]. Cerebellar input to the thalamus has been well established [33–35] and cerebellar projections could be implicated in the neuronal switch from burst into tonic mode. This switch has been hypothesized to alert cortical networks [36] and demonstrated to be central to performance in higher cognitive tasks [37]. Cerebellar projections via the thalamus to cortical regions are currently discussed to not purely serve movement but to also play an important role for cognition and emotion regulation [38]. Such behavioral changes have mostly been associated with lesions in areas of the posterior cerebellum [39]

that correspond to the cerebellar regions we find the strongest increase in connectivity induced by the SSRI.

While a role for serotonin has been well established in many stages of neuroplasticity, such as modulation of neural cell proliferation, migration, and differentiation as well as neurite outgrowth, axonal guidance, synaptogenesis, and efficiency of transsynaptic signaling [40], most of these effects are believed to require a long duration to occur. It has been postulated that the potential neuroplastic effects of antidepressants, such as the SSRIs, are expected to take several weeks to unfold [41], a time frame that nicely maps onto the period typically required to see an effective clinical response to this class of drugs [42]. However, several lines of evidence point toward the acute potential of an increase in extracellular serotonin to induce synaptoplastic effects, e.g., through the rapid activation of tropomyosin related kinase (Trk)-B-phospholipase-C (PLC)-1-cAMP response element-binding (CREB) signaling [43]. Most investigators interpret data indicating serotonin-induced changes in Trk signaling and brain-derived neurotrophic factor (BDNF) secretion as an acute mechanism, whereas serotonergic modulation of BDNF expression levels is considered a chronic process. Interestingly, there are also reports

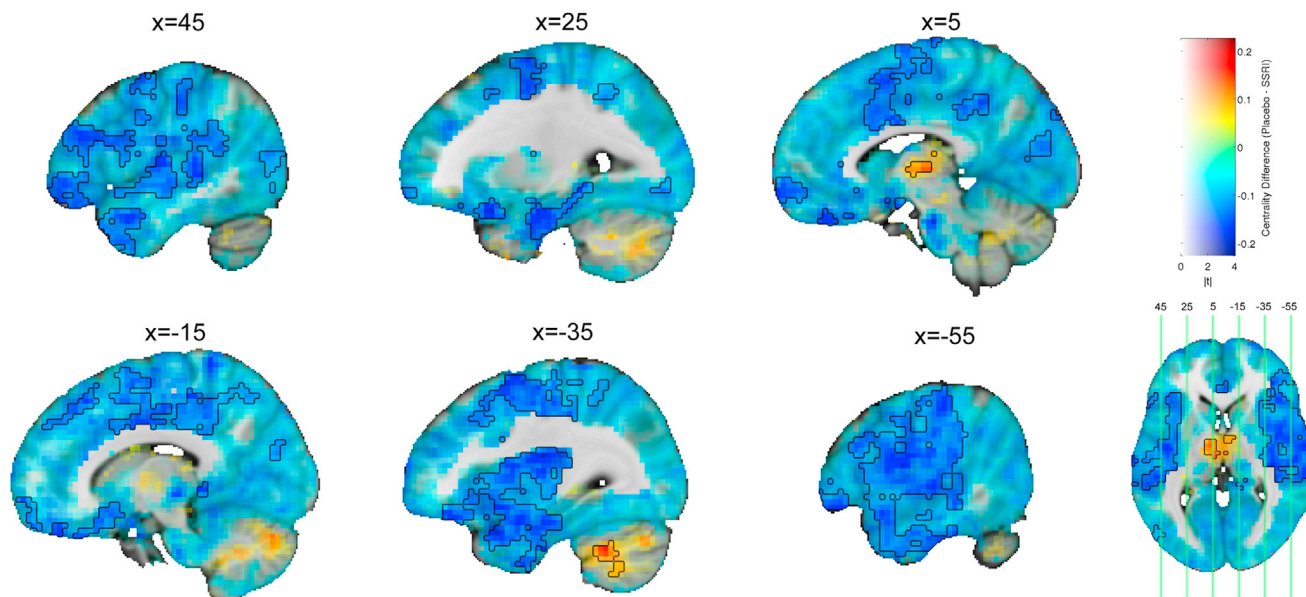


Figure 3. Signal Change in Degree Centrality Induced by a Single Dose of Escitalopram Contrasted with Placebo

Sagittal slices show the contrast of degree centrality between placebo and escitalopram condition superimposed on a T1-anatomical standard MNI template. Orange colors indicate increased centrality; blue colors decreased centrality following SSRI administration compared to placebo. Dark lines indicate significant clusters ($p < 0.01$, corrected for multiple comparisons). Significant increases in degree centrality are located in the thalamus and the cerebellum; decreases in degree centrality were found throughout the neocortex. Position of sagittal slices is shown in one axial slice. Table S1 provides a comprehensive overview of all significant clusters in the escitalopram versus placebo condition. Figure S3 depicts the contrast at a range of thresholds ($r > 0.10$, $r > 0.15$, $r > 0.20$).

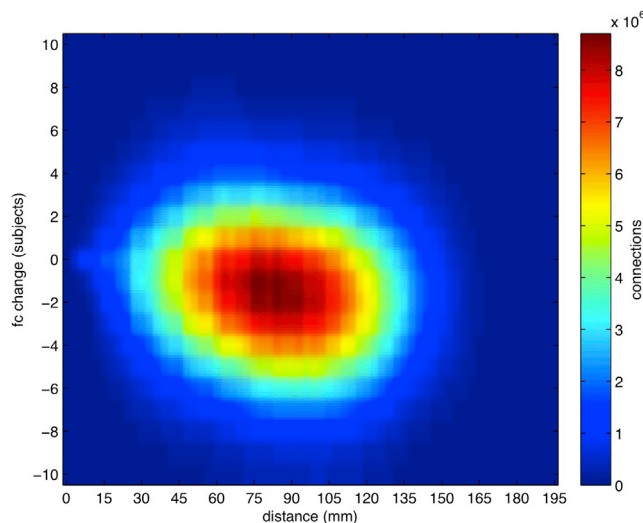


Figure 4. Change of Functional Connectivity between the Placebo and SSRI Condition and Euclidean Length of Connection

The x axis indicates the Euclidean distance (mm) between the two end-points of the respective connection. The y axis displays the mean functional connectivity difference (placebo-SSRI). The color indicates the number of connections, with hot colors reflecting a high number of connections with specific distance and change and blue colors indicating fewer connections. For further details on connectivity changes within and between network modules, see [Figures S1](#) and [S2](#).

that support an acute effect of serotonin on BDNF expression levels [44] and many questions remain unanswered regarding the timeline from initiation of a neuroplastic process to how long this process is sustained. Exploring functional connectivity changes that potentially reflect an early marker for neuroplastic change in vivo in the light of a serotonergic challenge thus seems a valuable strategy to conceptualize a model for the time frame of serotonergic action in the human brain.

Main Findings and Implications

We demonstrate an acute and widespread decrease in functional connectivity across the whole brain following the oral intake of a single dose of escitalopram in healthy subjects, as well as the change in connectivity not to be limited to a decrease but to be paralleled with localized increases in cerebellar and thalamic regions. These findings provide evidence for the particular relevance of serotonin for the modulation of intrinsic brain activity and also demonstrate its unique influence on the cerebello-thalamic tract. The observed link between rapid serotonin transporter blockade and such fundamental functional connectivity change across the whole brain suggests a very early initiation time for serotonin-induced modulation of functional connectivity architecture. While further research is needed to establish whether these serotonin-induced connectivity changes hold promise to translate into meaningful predictors for antidepressant response, our findings represent a first step toward identifying an intrinsic functional connectome print for individual responsiveness of the human brain to serotonergic modulation.

Supplemental Information

Supplemental Information includes three figures, one table, and Supplemental Experimental Procedures and can be found with this article online at <http://dx.doi.org/10.1016/j.cub.2014.08.024>.

Acknowledgments

The study was supported by the Society in Science—The Branco Weiss Fellowship to J.S. and the Max Planck Society.

Received: April 8, 2014

Revised: June 30, 2014

Accepted: August 13, 2014

Published: September 18, 2014

References

1. Frazer, A., and Hensler, J.H. (1999). Serotonin Involvement in Physiological Function and Behavior, Sixth Edition (Philadelphia: Lippincott-Raven).
2. McCabe, C., and Mishor, Z. (2011). Antidepressant medications reduce subcortical-cortical resting-state functional connectivity in healthy volunteers. *Neuroimage* 57, 1317–1323.
3. McCabe, C., Mishor, Z., Filippini, N., Cowen, P.J., Taylor, M.J., and Harmer, C.J. (2011). SSRI administration reduces resting state functional connectivity in dorso-medial prefrontal cortex. *Mol. Psychiatry* 16, 592–594.
4. van de Ven, V., Wingen, M., Kuypers, K.P., Ramaekers, J.G., and Formisano, E. (2013). Escitalopram decreases cross-regional functional connectivity within the default-mode network. *PLoS ONE* 8, e68355.
5. Jacobs, B.L., and Azmitia, E.C. (1992). Structure and function of the brain serotonin system. *Physiol. Rev.* 72, 165–229.
6. Holmes, A., Murphy, D.L., and Crawley, J.N. (2003). Abnormal behavioral phenotypes of serotonin transporter knockout mice: parallels with human anxiety and depression. *Biol. Psychiatry* 54, 953–959.
7. Scharinger, C., Rabl, U., Kasess, C.H., Meyer, B.M., Hofmaier, T., Diers, K., Bartova, L., Pail, G., Huf, W., Uzelac, Z., et al. (2014). Platelet serotonin transporter function predicts default-mode network activity. *PLoS ONE* 9, e92543.
8. Willeit, M., Sitte, H.H., Thierry, N., Michalek, K., Praschak-Rieder, N., Zill, P., Winkler, D., Brannath, W., Fischer, M.B., Bondy, B., et al. (2008). Enhanced serotonin transporter function during depression in seasonal affective disorder. *Neuropsychopharmacology* 33, 1503–1513.
9. Pirraglia, P.A., Stafford, R.S., and Singer, D.E. (2003). Trends in prescribing of selective serotonin reuptake inhibitors and other newer antidepressant agents in adult primary care. *Prim. Care Companion J. Clin. Psychiatry* 5, 153–157.
10. Artigas, F. (1993). 5-HT and antidepressants: new views from microdialysis studies. *Trends Pharmacol. Sci.* 14, 262.
11. Invernizzi, R., Velasco, C., Bramante, M., Longo, A., and Samanin, R. (1997). Effect of 5-HT_{1A} receptor antagonists on citalopram-induced increase in extracellular serotonin in the frontal cortex, striatum and dorsal hippocampus. *Neuropharmacology* 36, 467–473.
12. Muraki, I., Inoue, T., Hashimoto, S., Izumi, T., Ito, K., and Koyama, T. (2001). Effect of subchronic lithium treatment on citalopram-induced increases in extracellular concentrations of serotonin in the medial prefrontal cortex. *J. Neurochem.* 76, 490–497.
13. Brühl, A.B., Kaffenberger, T., and Herwig, U. (2010). Serotonergic and noradrenergic modulation of emotion processing by single dose antidepressants. *Neuropsychopharmacology* 35, 521–533.
14. Grady, C.L., Siebner, H.R., Hornboll, B., Macoveanu, J., Paulson, O.B., and Knudsen, G.M. (2013). Acute pharmacologically induced shifts in serotonin availability abolish emotion-selective responses to negative face emotions in distinct brain networks. *Eur. Neuropsychopharmacol.* 23, 368–378.
15. Loubinoux, I., Pariente, J., Boulanouar, K., Carel, C., Manelfe, C., Rascol, O., Celsis, P., and Chollet, F. (2002). A single dose of the serotonin neurotransmission agonist paroxetine enhances motor output: double-blind, placebo-controlled, fMRI study in healthy subjects. *Neuroimage* 15, 26–36.
16. Biswal, B., Yetkin, F.Z., Haughton, V.M., and Hyde, J.S. (1995). Functional connectivity in the motor cortex of resting human brain using echo-planar MRI. *Magn. Reson. Med.* 34, 537–541.
17. Biswal, B.B., Mennes, M., Zuo, X.N., Gohel, S., Kelly, C., Smith, S.M., Beckmann, C.F., Adelstein, J.S., Buckner, R.L., Colcombe, S., et al. (2010). Toward discovery science of human brain function. *Proc. Natl. Acad. Sci. USA* 107, 4734–4739.

18. Keller, C.J., Bickel, S., Honey, C.J., Groppe, D.M., Entz, L., Craddock, R.C., Lado, F.A., Kelly, C., Milham, M., and Mehta, A.D. (2013). Neurophysiological investigation of spontaneous correlated and anti-correlated fluctuations of the BOLD signal. *J. Neurosci.* 33, 6333–6342.
19. Nir, Y., Mukamel, R., Dinstein, I., Privman, E., Harel, M., Fisch, L., Gelbard-Sagiv, H., Kipervasser, S., Andelman, F., Neufeld, M.Y., et al. (2008). Interhemispheric correlations of slow spontaneous neuronal fluctuations revealed in human sensory cortex. *Nat. Neurosci.* 11, 1100–1108.
20. Zuo, X.N., Ehmke, R., Mennes, M., Imperati, D., Castellanos, F.X., Sporns, O., and Milham, M.P. (2012). Network centrality in the human functional connectome. *Cereb. Cortex* 22, 1862–1875.
21. Aronson, S., and Delgado, P. (2004). Escitalopram. *Drugs Today (Barc)* 40, 121–131.
22. Dieudonné, S., and Dumoulin, A. (2000). Serotonin-driven long-range inhibitory connections in the cerebellar cortex. *J. Neurosci.* 20, 1837–1848.
23. Avesar, D., and Gullledge, A.T. (2012). Selective serotonergic excitation of callosal projection neurons. *Front Neural Circuits* 6, 12.
24. Smith, S.M., Fox, P.T., Miller, K.L., Glahn, D.C., Fox, P.M., Mackay, C.E., Filippini, N., Watkins, K.E., Toro, R., Laird, A.R., and Beckmann, C.F. (2009). Correspondence of the brain's functional architecture during activation and rest. *Proc. Natl. Acad. Sci. USA* 106, 13040–13045.
25. Buckner, R.L., Krienen, F.M., and Yeo, B.T. (2013). Opportunities and limitations of intrinsic functional connectivity MRI. *Nat. Neurosci.* 16, 832–837.
26. Sporns, O. (2014). Contributions and challenges for network models in cognitive neuroscience. *Nat. Neurosci.* 17, 652–660.
27. Kugelberg, F.C., Apelqvist, G., Carlsson, B., Ahlner, J., and Bengtsson, F. (2001). In vivo steady-state pharmacokinetic outcome following clinical and toxic doses of racemic citalopram to rats. *Br. J. Pharmacol.* 132, 1683–1690.
28. Kugelberg, F.C., Carlsson, B., Ahlner, J., and Bengtsson, F. (2003). Stereoselective single-dose kinetics of citalopram and its metabolites in rats. *Chirality* 15, 622–629.
29. Mayberg, H.S., Brannan, S.K., Tekell, J.L., Silva, J.A., Mahurin, R.K., McGinnis, S., and Jerabek, P.A. (2000). Regional metabolic effects of fluoxetine in major depression: serial changes and relationship to clinical response. *Biol. Psychiatry* 48, 830–843.
30. Baldinger, P., Kranz, G.S., Haeusler, D., Savli, M., Spies, M., Philippe, C., Hahn, A., Höflich, A., Wadsak, W., Mitterhauser, M., et al. (2014). Regional differences in SERT occupancy after acute and prolonged SSRI intake investigated by brain PET. *Neuroimage* 88, 252–262.
31. Nord, M., Finnema, S.J., Halldin, C., and Farde, L. (2013). Effect of a single dose of escitalopram on serotonin concentration in the non-human and human primate brain. *Int. J. Neuropsychopharmacol.* 16, 1577–1586.
32. Moore, R.Y., Halaris, A.E., and Jones, B.E. (1978). Serotonin neurons of the midbrain raphe: ascending projections. *J. Comp. Neurol.* 180, 417–438.
33. Asanuma, C., Thach, W.T., and Jones, E.G. (1983). Distribution of cerebellar terminations and their relation to other afferent terminations in the ventral lateral thalamic region of the monkey. *Brain Res.* 286, 237–265.
34. Stanton, G.B. (1980). Topographical organization of ascending cerebellar projections from the dentate and interposed nuclei in *Macaca mulatta*: an anterograde degeneration study. *J. Comp. Neurol.* 190, 699–731.
35. Thach, W.T., and Jones, E.G. (1979). The cerebellar dentatothalamic connection: terminal field, lamellae, rods and somatotopy. *Brain Res.* 169, 168–172.
36. Kim, U., and McCormick, D.A. (1998). The functional influence of burst and tonic firing mode on synaptic interactions in the thalamus. *J. Neurosci.* 18, 9500–9516.
37. Law, N., Bouffet, E., Laughlin, S., Laperriere, N., Brière, M.E., Strother, D., McConnell, D., Hukin, J., Fryer, C., Rockel, C., et al. (2011). Cerebello-thalamo-cerebral connections in pediatric brain tumor patients: impact on working memory. *Neuroimage* 56, 2238–2248.
38. Schmahmann, J.D., and Pandya, D.N. (2008). Disconnection syndromes of basal ganglia, thalamus, and cerebrocerebellar systems. *Cortex* 44, 1037–1066.
39. Schmahmann, J.D., and Sherman, J.C. (1998). The cerebellar cognitive affective syndrome. *Brain* 121, 561–579.
40. Azmitia, E.C., and Whitaker-Azmitia, P.M. (1997). Development and adult plasticity of serotonergic neurons and their target cells. In *Serotonergic Neurons and 5-HT Receptors in the CNS*, H.G. Baumgarten and M. Göthert, eds. (Berlin: Springer), pp. 1–39.
41. Castrén, E. (2005). Is mood chemistry? *Nat. Rev. Neurosci.* 6, 241–246.
42. Nestler, E.J. (1998). Antidepressant treatments in the 21st century. *Biol. Psychiatry* 44, 526–533.
43. Rantamäki, T., Hendolin, P., Kankaanpää, A., Mijatovic, J., Piepponen, P., Domenici, E., Chao, M.V., Männistö, P.T., and Castrén, E. (2007). Pharmacologically diverse antidepressants rapidly activate brain-derived neurotrophic factor receptor TrkB and induce phospholipase-Cgamma signaling pathways in mouse brain. *Neuropsychopharmacology* 32, 2152–2162.
44. Zetterström, T.S., Pei, Q., Madhav, T.R., Coppel, A.L., Lewis, L., and Grahame-Smith, D.G. (1999). Manipulations of brain 5-HT levels affect gene expression for BDNF in rat brain. *Neuropharmacology* 38, 1063–1073.

Current Biology, Volume 24

Supplemental Information

Serotonergic Modulation of Intrinsic Functional Connectivity

Alexander Schaefer, Inga Burmann, Ralf Regenthal, Katrin Arélin, Claudia Barth, André Pampel, Arno Villringer, Daniel S. Margulies, and Julia Sacher

Supplemental Information

1. Supplemental Data

Figure S1

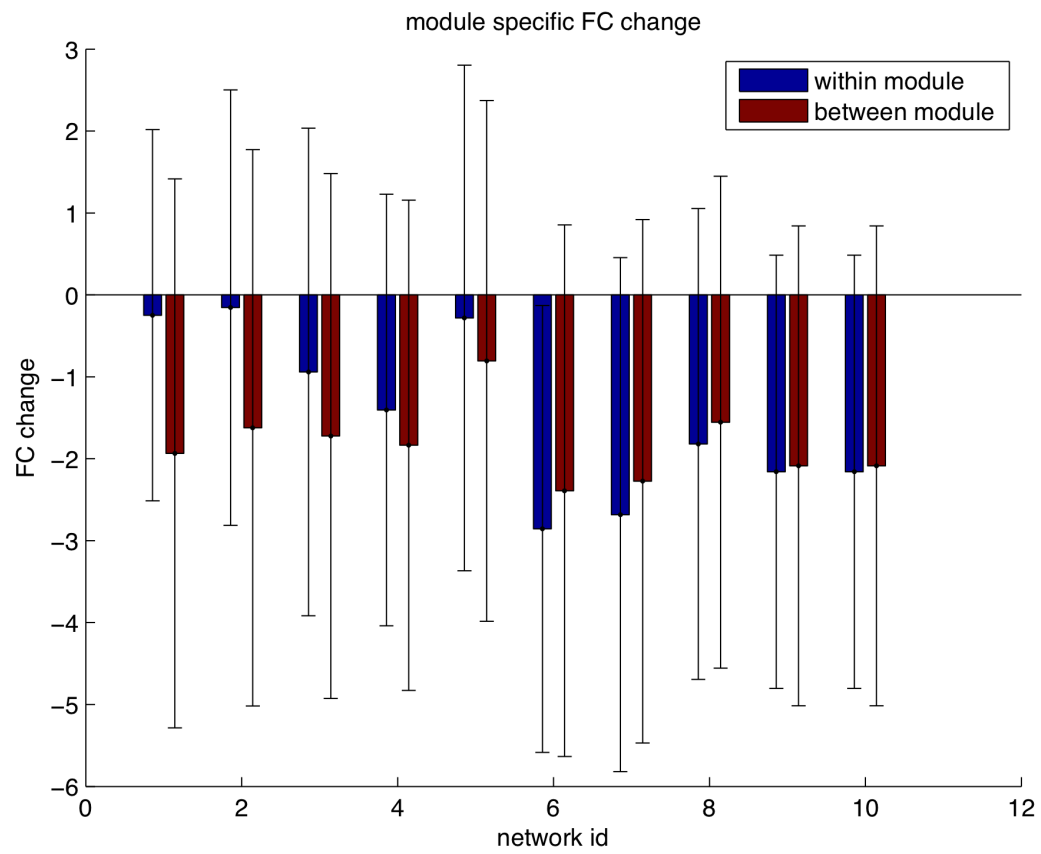


Figure S2

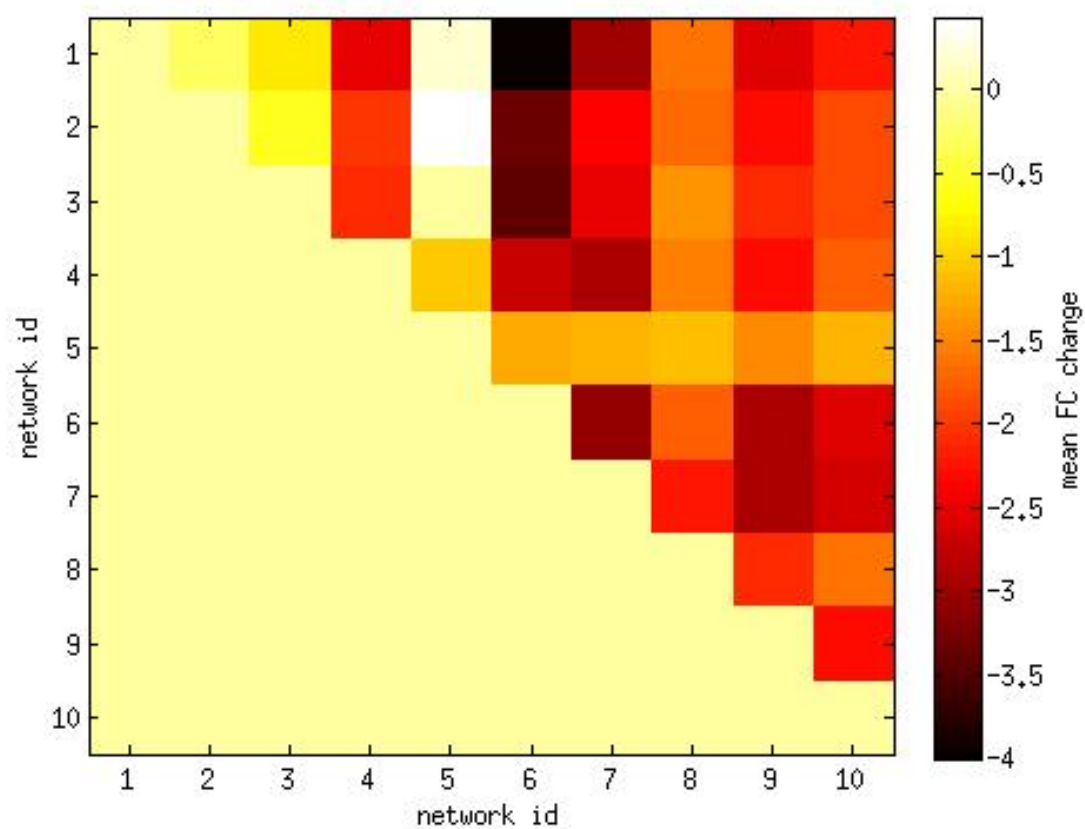
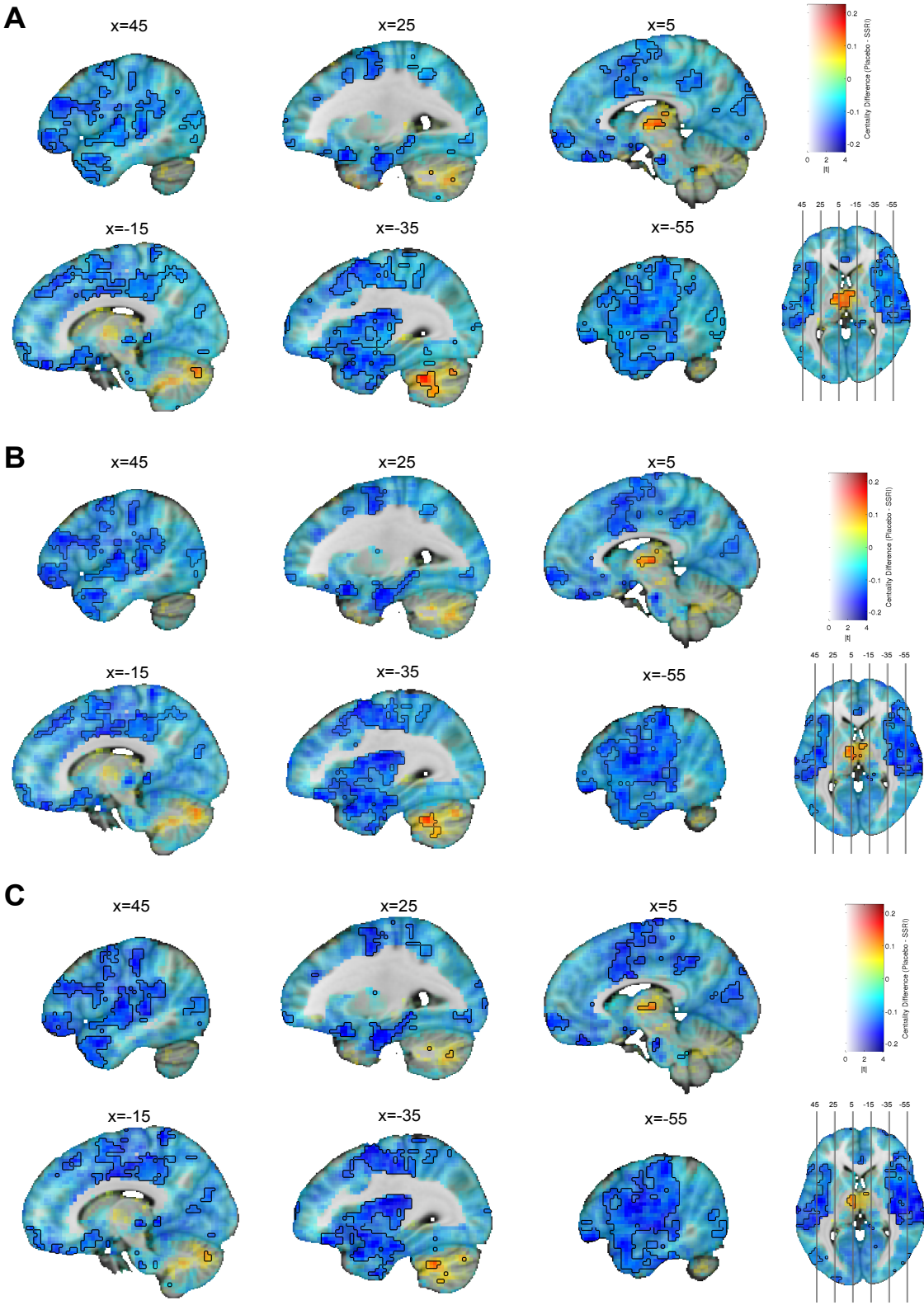


Figure S3



Legends

Figure S1 Change of functional connectivity (FC) between the placebo and SSRI condition (placebo-SSRI) within and between ten major network-modules [S1]. The labels for network-IDs shown on the x-axis correspond to the respective networks in Figure 1 of the Smith et al study. The y-axis indicates functional connectivity (mean \pm SD) for within-module change (blue) and between-module change (red) for the contrast placebo versus SSRI.

Figure S2 Between-module changes of functional connectivity (FC) for the placebo and SSRI condition. The x-axis and y-axis indicate the network id [S1]. FC difference (placebo-SSRI) of connections between the respective modules is displayed as intensity on a color-scale. Red and dark colors indicate a strong reduction; lighter colors indicate a weaker reduction.

Figure S3 Sagittal slices show the contrast of degree centrality with a threshold of $r > 0.10$ (Panel A), $r > 0.15$ (Panel B), and $r > 0.20$ (Panel C) between placebo and escitalopram conditions superimposed on a T1-anatomical standard MNI template. Orange colors indicate increased centrality blue colors decreased centrality following SSRI-administration compared to placebo. Black lines indicate significant clusters ($p < 0.01$, corrected for multiple comparisons). Significant increases in degree centrality are located in the thalamus and the cerebellum, decreases in degree centrality were found throughout most cortical and subcortical regions.

Table S1_Significant differences between brain states following a single dose of escitalopram versus placebo using degree centrality mapping.

List of clusters illustrating significant decreases and increases in degree centrality corrected for multiple comparisons at $p < 0.01$. Only clusters larger than 45 voxels are listed. Coordinates of the peak DC intensity are listed in MNI standard space.

Cluster #	T-value (mean \pm SM)	Regions	Volume (mm ³)	Coordinates	Change of direction
1	3.44 \pm 0.005	Right Superior Temporal Gyrus, Right Inferior Temporal Gyrus, Left Superior Temporal Gyrus, Right Precentral Gyrus, Right Postcentral Gyrus, Right Insula, Right Middle Temporal Gyrus, Left Insula, Left Middle Frontal Gyrus, Left Middle Temporal Gyrus	262602	(36,-38,-19)	Decrease
2	3.45 \pm 0.038	Right Superior Frontal Gyrus	6858	(18,51,-22)	Decrease
3	3.11 \pm 0.019	Left/Right Cuneus	4077	(15,-81,15)	Decrease
4	3.46 \pm 0.046	Left Middle Temporal Gyrus, Left Superior Temporal Gyrus	3348	(-6,72,-7)	Decrease
5	3.52 \pm 0.073	Right semilunar lobule (lateral Crus II)	2538	(39,-51,-46)	Increase
6	3.24 \pm 0.032	Inferior Occipital Gyrus, Middle Occipital Gyrus	2511	(-58,-74,-11)	Decrease
7	3.10 \pm 0.023	Left Superior Parietal Lobule, Left Inferior Parietal Lobule	2268	(-30,-58,52)	Decrease

8	3.12±0.028	Right Anterior Cingulate Gyrus, Left Anterior Cingulate Gyrus	2025	(0,43,-1)	Decrease
9	3.52±0.064	Left Thalamus, Right Thalamus	1701	(0,-22,12)	Increase
10	3.40±0.063	Right Parahippocampal Gyrus	1377	(12,-37,-2)	Decrease

2. Supplemental Experimental Procedures

Methods

Participants

Data from twenty-two right-handed participants (11 female, mean age= 25±2 s.d.) were included in the analysis (two additional participants were excluded because of technical problems) after we obtained written informed consent. Subjects were free from any general medical, neurological or psychiatric illness. Participants were screened using the Structured Clinical Interview for DSM IV [S2] to disqualify any Axis I major mental disorders supplemented by the exclusion from Axis II personality disorders, the Hamilton Depression Scale (HAM-D) [S3], the self-report version of the Structured Clinical Interview for Mood Spectrum (MOODS-SR) [S4] for subclinical manic symptoms, and Spielberger State-Trait Anxiety Inventory (STAI) [S5] scores. All subjects were antidepressant-naïve and medication-free except for the contraceptive pill. Additionally, participants were non-smokers and had no history of alcohol or any other substance abuse. All study-procedures were approved by the institutional review board of the University of Leipzig.

Study drug protocol

The study was conducted according to a double-blind, placebo controlled, two-way cross-over design. Complete balancing of the treatments was conducted by two treatment orders which were randomly assigned to participants (for overview, see Figure 1). Study-drug administration consisted of a single dose of escitalopram (20 mg) and placebo administered at two different test days separated by a wash-out period of eight weeks. MRI scanning was scheduled during the maximum concentration of escitalopram in blood (C_{max}) between 3-4 hours [S6] after drug-administration, a blood sample was taken prior to scanning. Before each scan, a self-report assessment of alertness, mood, calmness, anxiety, strength, concentration, coordination, energy, attention, sociability, and self-confidence (visual analogue scales [VAS] [S7]) was conducted.

Escitalopram Levels

Serum values of escitalopram (nanograms per milliliter) were determined with liquid chromatography with UV-detection. The limit of quantification for escitalopram was 1 ng/ml.

Image acquisition

Structural and functional MRI data were acquired on a Siemens Verio 3 Tesla Scanner at the Dayclinic for Cognitive Neurology, University of Leipzig, equipped with a 32-channel head coil. The scans consisted of an anatomical T1 weighed sequence and a T2 weighed resting-state fMRI scan. The structural T1 scan took approximately 10 minutes extended by a resting-state T2 EPI sequence of 15 minutes. For the resting-state scan 410 volumes were acquired using the following

parameters: TR=2200ms, TE=30ms, flip angle=90⁰, 34 slices with a resolution of 3x3x4.3 mm³. Volunteers were instructed to focus on a fixation cross while not thinking about anything in particular and not falling asleep. After completion of the baseline scan the SSRI or placebo were administered in a double-blind randomized design. Three hours post-medication the second T2 resting-state scan was acquired.

Image preprocessing

The preprocessing of resting-state fMRI data was carried out using both FSL [S8] and AFNI [S9]. The steps included: 1) discarding the first four EPI volumes from each resting-state scan to allow for signal equilibration, 2) 3D motion correction, 3) time series despiking, 4) 6 mm Full Width Half Maximum spatial smoothing, 5) 4D mean-based intensity normalization, 6) band-pass temporal filtering (0.01-0.1 Hz), 7) removing linear and quadratic trends and, 8) regressing out eight nuisance signals (white matter, cerebrospinal fluid and six motion parameters). The output of these preprocessing steps was one 4D residual functional volume for each participant. The linear normalization of the functional volume to Montreal Neurological Institute (MNI) space [S10] was performed using FSL with the individual T1 as a prior.

Functional Connectivity Analysis

To perform high dimensional connectivity analysis we used the computational efficient degree centrality implementation in LIPSIA [S11]. The preprocessed resting-state fMRI data in MNI space was converted from NIFTI format to LIPSIA's vista format. To include only grey matter voxels we thresholded the ICBM152 grey matter template [S10] at 0.25 or 25% resulting in a gray matter mask of 63046 voxels. To calculate degree centrality we created a connectivity matrix with 63046 nodes where

each node represents one voxel. Degree centrality measures connectivity by counting the number of connections of each specific node. This number is then assigned as a centrality value to the given node. To count connections a threshold needs to be applied. We used $r > 0.15$ as a threshold for including connections in our analysis. After calculating degree centrality for each voxel we converted LIPSIAs' vista images back into the NIFTI format. Statistical testing on the resulting NIFTI images was performed in AFNI using 3dttest++. The resulting images were thresholded with $p < 0.01$ on a voxel and cluster level. The minimum cluster size of 45 voxels was computed using AlphaSim, a Monte Carlo simulation tool implemented in AFNI, to correct for multiple comparisons.

3. Supplemental References

- S1. Smith, S.M., Fox, P.T., Miller, K.L., Glahn, D.C., Fox, P.M., Mackay, C.E., Filippini, N., Watkins, K.E., Toro, R., Laird, A.R., et al. (2009). Correspondence of the brain's functional architecture during activation and rest. *Proc Natl Acad Sci U S A* 106, 13040-13045.
- S2. First, M.S., R; Willimas, J; Gibbon, M (1995). Structured Clinical Interview for DSM-IV Axis I Disorders, Patient Edition (SCID-P). In Biometrics Research, Volume Version 2. (New York, NY).
- S3. Hamilton, M. (1960). A rating scale for depression. *Journal of Neurology, Neurosurgery and Psychiatry* 23, 56-62.
- S4. Dell'Osso, L., Armani, A., Rucci, P., Frank, E., Fagiolini, A., Corretti, G., Shear, M.K., Grochocinski, V.J., Maser, J.D., Endicott, J., et al. (2002). Measuring mood spectrum: comparison of interview (SCI-MOODS) and self-report (MOODS-SR) instruments. *Comprehensive psychiatry* 43, 69-73.
- S5. Spielberger, C., and Vagg, P. (1984). Psychometric properties of the STAI: A reply to Ramanaiah, Franzen, and Schill. *Journal of Personality Assessment* 48, 95-97.
- S6. Aronson, S., and Delgado, P. (2004). Escitalopram. *Drugs of today* 40, 121-131.
- S7. Bond, A., and Lader, M. (1974). The use of analogue scales in rating subjective feelings. *British Journal of Medical Psychology* 47, 211-218.
- S8. Jenkinson, M., Beckmann, C.F., Behrens, T.E., Woolrich, M.W., and Smith, S.M. (2012). *Fsl. Neuroimage* 62, 782-790.
- S9. Cox, R.W. (1996). AFNI: software for analysis and visualization of functional magnetic resonance neuroimages. *Comput. Biomed. Res.* 29, 162-173.
- S10. Mazziotta, J.C., Toga, A.W., Evans, A., Fox, P., and Lancaster, J. (1995). A probabilistic atlas of the human brain: theory and rationale for its development. The International Consortium for Brain Mapping (ICBM). *Neuroimage* 2, 89-101.
- S11. Lohmann, G., Muller, K., Bosch, V., Mentzel, H., Hessler, S., Chen, L., Zysset, S., and von Cramon, D.Y. (2001). LIPSIA--a new software system for the evaluation of functional magnetic resonance images of the human brain. *Comput. Med. Imaging Graph.* 25, 449-457.